Central composite design based electrocoagulation process for the treatment of textile effluent of S.I.T.E, industrial zone of Karachi City

Abdul Rauf Shah, Hajira Tahir*, H.M. Kifayatullah

Department of Chemistry, University of Karachi, 75270, Karachi, Pakistan, email: raufshah32@yahoo.com (A. RaufShah), hajirat@uok.edu.pk (H. Tahir), hafizkif@yahoo.com (H.M. Kifayatullah)

ABSTRACT

In the present research work, it found that the Electrocoagulation Process (EC) could be effectively utilized for the purification of tri-dye (Yellow 145, Reactive Red 195, and Blue 222) from wastewater of the textile industry located in Karachi. In order to purify the sample from the said dyes, the impacts of operational parameters namely pH, electrolysis time, amount of electrolyte and voltage were monitored on color and COD (chemical oxygen demand) removals potency using central composite design (CCD). As a result of this, the electrolysis time and amount of electrolyte showed a greater influence on color and COD removals than pH and voltage. The R^2 (regression coefficient) values of the effluent was observed from 87% to 98% by ANOVA (Analysis of Variance). Subsequently, the kinetic reaction was also determined in the discharge of industry. Simultaneously, The Fourier transform infrared (FTIR) analysis was performed to identify the presence of functional groups of the dyes contaminated in the sample. Afterwards, the inverse relation was observed between the concentration of NaCl and the specific electrical energy consumption (SEEC). Consequently, the sludge formation of tri-dyes was obtained from sample and then calculated. By this, the industrial effluent was filtered from three harmful dyes that can be very dangerous for human as well as aquatic life. Moreover, it is cost effective technique too because its operating cost is US$ 1.360/L. Hence, this method may be used as a purifier for effluents of textile industries.

Keywords: Electrocoagulation process; Central Composite Design; Kinetic study; Specific electrical energy consumption (SEEC); FTIR

1. Introduction

Industrialization is considered a key factor for the economic growth in a country. The environmental pollution is one of the major problems, currently facing in the world. It produces substantial amount of wastewater, that containing color, suspended particles, non-biodegradable materials and high chemical oxygen demand (COD). They collectively cause the severe water pollution and lead to toxic and carcinogenic effects on genetic level in living organisms. The contaminated tri-dye in effluent obstruct the light diffusion in the water of lakes and rivers [1–3]. Over 10,000 dyes with an annual production of greater than 7×10^5 metric tons are commercially available [4,5].

Around up to 50% of these dyes are lost subsequent to the dyeing process and disposed out in the effluent [6]. Moreover, the reactive dyes are generally used industrially. They need a world market share about 60–70% [4,5]. The release of colored effluents into the aquatic ecosystem promotes environmental and public health risks because of their negative ecotoxicological effects and bioaccumulation in wildlife [7]. To remove the contaminants, various methods have already been designed [8]. The ever increasing customary of drinking water supply and also demanding environmental rules the electrochemical technologies have regained their worldwide importance [9]. The (EC) processes are taken into account as an efficient tool for the treatment of industrial wastewaters with high removal efficiencies [10]. Moreover, the EC is a simple and efficient process where the production of the coagulating agent is managed in situ by means of electrooxidation of sacrificial

---

*Corresponding author.

anodes [11]. The work done by former researchers is showing that the EC process has proposed is as an effective method of treating diverse effluents such as textile wastewater, paper mill wastewater, urban wastewater, laundry wastewater, nitrate and phosphate bearing wastewater, electroplating wastewater and chemical mechanical polishing wastewater, etc. [2,12–14]. Indeed, the interaction among the coagulant and the pollutant is the generally complicated aspect of the EC process [15]. Furthermore, the EC process combines three main interdependent processes: operating synergistically to remove pollutants including electrochemistry, coagulation and hydrodynamics [16]. Bestowing to [17–19], the various stages involved in the EC process are considering the migration to an oppositely charged electrode (electrophoresis) and aggregation due to charge neutralization. Additionally, the metallic cations interact with OH– to form a hydroxide, which have high adsorption property. Consequently, it bonds with the pollutant; the removal process by electro floatation, sedimentation and adhesion was also assessed [20,21].

During the EC process, numerous reactions take place at the surface of electrodes, especially dissolution of aluminum through oxidation of anode, and at the same time it cause's reduction of water to form hydrogen gas. The breakdown of water that occurs represent as:

At cathode:

$$2H_2O + 2e^- \rightarrow H_2 + 2OH^- \tag{1}$$

At anode:

$$Al \rightarrow Al^{+3} + 3e^- \tag{2}$$

$$2H_2O \rightarrow 4H^+ + O_2 + 4e^- \tag{3}$$

The nascent Al^{3+} ions are very efficient coagulants for particles flocculation. Despite the fact the hydrolyzed aluminium ions can form large networks of Al–O–Al–OH that can chemically adsorb pollutants [22]. It chemically induces the aluminium and its hydroxide film and it is represented by the following reaction [Eq. (5)] [23,24].

$$2Al + 6H_2O + 2OH^- \rightarrow 2Al(OH)_4^- + 3H_2 \tag{4}$$

$$2Al + 3H_2O \rightarrow 2Al^{+3} + 3/2H_2 + 3OH^- \tag{5}$$
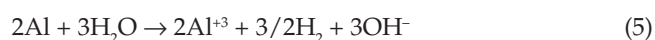
In addition to this, the $Al(OH)_4^-$ ions are liberated during a chemical reaction and they are able to react with cationic species to eliminate pollutants from effluent. So,they neutralize their charges and reduce their solubility [9].

$$[Al(OH)_4^-] \rightarrow Al(OH)_3 + OH^- \tag{6}$$
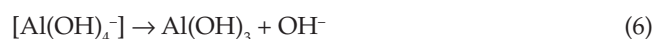
The Response Surface Methodologies (RSM) typically applied in experimental design. The Box–Behnken is a spherical rotational design that requires an experimental number ($N = k^2 + k + cp$). It is used for many physical and chemical processes improvement. Moreover, its application in analytical chemistry is far less than the Doehlert matrix design and central composite design (CCD) [25]. The RSM was employed to design the experiments by Minitab 17 software.

2. Materials and methods

2.1. Protocol of experiment

2.1.1. Textile industrial effluent samples collection and treatment

The wastewater was collected from textile industry of Karachi, Pakistan. The EC process was designed at laboratory scale frame work. The EC process setup is represented in (Fig. 1). The EC experiments were carried out in 1000 mL cylindrical glass reactor and magnetically stirred it by (78HW-1 serial constant-temperature magnetic pug mill) for industrial run-off. The aluminium and iron electrodes were used as anode and cathode, respectively. Moreover, geometrically they were sheet in outline. All the experiments were done at room temperature. Approximately, 1000 mL of discharged effluent was utilized as a part of each run. The weights of the compounds were measured by Adventure Oahu's Digital Weighing Balance Model AR2140, whereas, pH, TDS, conductance and temperature of textile effluent were monitored by portable pH/EC/TDS/temperature HANNA, H19811-5. The absorbance measurements were performed by UV/VIS spectrophotometer T80 (PG instruments, Ltd). Whereas, FTIR model NICOLET 67000 was used to study the structure of dyes. The EC experiments were proceeded and after each run the electrodes were cleaned with acetone and HCl (35%) to remove surface impurities [26].

The COD analysis was performed by standard colorimetric method. Moreover, the Standard Methods for the Examination of Water and Wastewater (APHA, 1992) were adopted for the determination of COD [27]. The absorbance of samples was analyzed byT80 UV/VIS spectrometer. After adjusting pH to the desirable value using NaOH and H_2SO_4, the samples were labeled and preserved as per standards method mentioned in Handbook of Water Analysis [28].

Tables 1 and 2 represents the characteristics of tri-dyes present in textile wastewater.

2.2. Electrocoagulation procedure

Towards the beginning of each trial, the fresh solution of effluent was transfered to 1000 mL glass reactor. The EC reactor was connected to the digital DC power supply (Yaxun 1502DD; 15V, 2A) equipped with galvanostatic operational choices. The values of sampling time of the treated wastewater was ranged as per designed model electrolysis time (min). The EC process samples were ejected from the electrochemical reactor. After that, they were filtered and
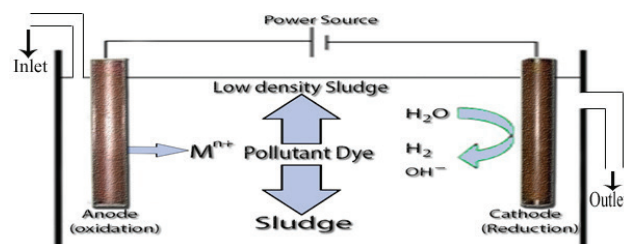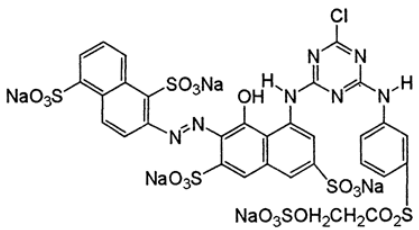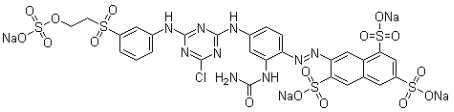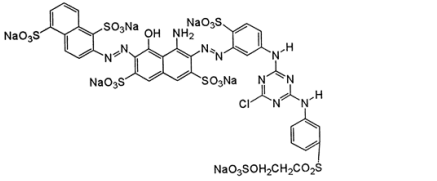

Fig. 1. Schematic representation of the experimental set up design for EC process.

Table 1
Physiochemical characterization of textile industrial effluent after dyeing process

Characteristics	Before EC process
Odor	Odorless
Color	Violet color
Turbidity	Less turbid
Conductance	>8 mS
pH	10.5–10.7
TDS	>8000 mg/L
Temperature	35–37°C
λ_{max}	511 nm, 541 nm, 668 nm
COD mg/L	2000–2500 mg/L
Absorbance	2–2.5 A
TSS	290 mg/L
Hardness	130 mg/L

Table 2
The characteristics of dyes present in textile wastewater

Dyes name	Molecular structure	λ_{max} (nm)
Red 195		541
Yellow 145		511
Blue 222		668

analyzed at respective dye λ_{max} by T80 UV/VIS spectrophotometer. The removal potency of three dyes was computed once and further statistical methods were applied. Whereas, the textile industrial effluents was treated at room temperature [28].

2.2.1. Standard curve method

The standard calibration method was applied for quantitative analysis of dyes in effluent. Moreover, the standard solutions were prepared ranging from 10–80 ppm and their absorbance were measured at their respective wavelengths using UV/VIS photometer.

2.2.2. Fourier transform (FTIR) studies

The sludge formed during the EC process. It was scanned by FTIR technique. The spectrum takes clue about the functional groups in the dye of textile discharge.

2.2.3. Total solids (TS) determination

Total solids were determined by gravimetric method and correspondingly then suspended and dissolve solids were also calculated represented as:

$$TS = TDS + TSS \tag{7}$$

2.2.4. Total hardness of the wastewater samples

The total hardness of the effluent samples was determined by EDTA titration method. For this purpose, 50 mL of sample was well mixed with 1–2 mL buffer of pH 10 and after that added a pinch of Eriochrome black-T indicator. The contents were titrated with 0.01 M EDTA till wine red solution change to blue. It was calculated by using following Eq. (8):

$$\text{Total hardness} = C \times D \times 1000 / \text{Volume} \tag{8}$$

where C represent volume (mL) of EDTA for titration, D (mg) of $CaCO_3$ equivalent to 1 mL of EDTA.

2.3. Determination of % color and chemical oxygen demand (COD) removal efficiencies

The removal efficiencies of dyes were calculated by the following equation:

$$(\%) \text{ Removal efficiency} = \frac{X_o - X_t}{X_o} \cdot 100 \tag{9}$$

X_o represents the initial values of dyes concentration and X_t represents the concentration of dyes in EC system after a certain electrolysis time (t).

COD removal values were deliberated by the following equation:

$$\% \text{ COD Removal} = \frac{[COD]_{initial} - [COD]_t}{[COD]_{initial}} \cdot 100 \tag{10}$$

where $[COD]_{initial}$ and $[COD]_t$ represent the before and after EC process at assured electrolysis interval time (t).

Table 3 represents the classification of compounds that contributes to COD [29].

2.4. Kinetic studies

The rate of reaction for the removal of color from textile discharge has been studied to exploit first-order kinetics. It is represented by Eq. (11).

$$\ln[A]_t = \ln A_o - k \cdot t \tag{11}$$

The rate constant k at time t can be estimated from the plot of vs. EC time t [30,31].

Table 3
Classification of compounds that contribute to COD

Classification	Types	
Organic compound	Suspended solids and liquids	Microorganism, colloids, emulsions, fat, oil, grease
	Miscible liquid	Alcohols, benzene, glycerin, oils
	Dissolved solids	Acids, salts, sugar
Inorganic compound	Dissolved	Cations: metals (Fe), metalloids (As)
		Anions: CN^-, NO_2^-, SO_3^-, S^{-2}

2.5. Response surface methodology (RSM) analysis

The experimental runs were performed according to CCD based on RSM [32]. The factors pH, electrolysis time, amount of electrolyte, and voltage were optimized. In a full factorial experimental design, the responses were measured at all combinations of the experimental factor levels [33]. The quadratic regression model was employed to predict the optimum conditions. The response (Y) can be expressed as polynomial model [34,35]. The coefficients were calculated by polynomial model as represented in Eq. (12):

$$Y = \beta_o + \sum_{i=1}^{4} \beta_i x_i + \sum_{i=1}^{4}\sum_{j=1}^{4} \beta_{ij} x_i x_j + \sum_{i=1}^{4} \beta_{i1} x_i^2 \qquad (12)$$

where Y is the predicted response and considered as a dependent variable. The X_i and X_j show the independent variables. β_0 is the constant coefficient, and β_i, β_{ij} and β_{ii} are the coefficients of linear, interaction and quadratic term, respectively. The analysis of variance (ANOVA) was used for graphical analysis of data to obtain the interaction between factors and responses. The quality of the fitted polynomial model was expressed by the regression coefficients R^2, and its statistical significance was checked by the Fisher's F-test [21].

3. Results and discussion

The interactive effects of variables on the responses, and 3D response surface plots are created for tri-dyes system. Figs. 2–4 indicate the removal potency of respective dyes.

3.1. Main effects plot

The parallel lines in interactions plots Fig. 5 show that there is no interaction. They conjointly represent the response for each factor level. The main effect observed on X-axis are not horizontal, and it represents the majority of impacts on the responses. The steeper slope of the line shows the greater magnitude of the main effect. The main effects on plot not only show the interactions but also looks at the interactions between factors.

3.2. Optimization of parameters

Figs. 6a,b are the optimized values that are found by software after performing designed experimental runs. They are showing predicted responses at optimum values. So, the experiments are performed at optimum values and responses are determined and compared with predicted responses. Hence, one can prove that Response Surface Methodology has been successfully proved for the optimization of process variables.

The surface plots of % COD removal efficiency as a function of operating parameters are represented in Fig. 7.

3.3. Effect of variables on % color removal potency

3.3.1 Influence of pH

The pH is a crucial variable that influences on EC process [36]. The decolorization efficiency was investigated by varying pH ranges from 3 to 9 as shown in Figs. 2–4. Though the pH between 5–7 then monomeric cationic species are evolved and converted to polymeric species such as $Al_2(OH)_2^{4+}$ and $Al_6(OH)_{15}^{3+}$ [9,26]. Furthermore, the flocculation process is followed at low pH ranges and it is explained by precipitation process. Even though the high pH more than >6.5 favors the adsorption process [37–39]. The pH > 9, shows the presence of $Al(OH)_4^-$ species within the system. These flocs are formed during the process are depicted as:

$$nAl(OH)_3 \rightarrow Al_n(OH)_{3n} \qquad (13)$$

Furthermore, the variation in pH has been observed by researchers and described the influence of pH on the process [40,41]. The increase in pH causes the hydrogen evolution at the cathode as represented in Eq. (14):

$$2H_2O + 2e^- \rightarrow H_2 + 2OH^- \qquad (14)$$

3.3.2. The influence of the electrolysis time

In EC process, Al/Fe combinations are effective for color and COD removals from wastewater [42]. Moreover, electrolysis time is significant operational parameter, and the higher operating time results in the higher energy requisite. Consequently, the outcome of operational parameter observed by %removal efficiency as represented in Figs. 2–4. The higher operation time causes the anodic passivation and cathodic polarization which hinders the efficiency of EC treatment process [43,44].

3.3.3. The influence of the amount of electrolyte

The increase in salt concentration decreases the voltage at constant current density and also reduces energy consumption [45,46]. The removal rate was observed to be
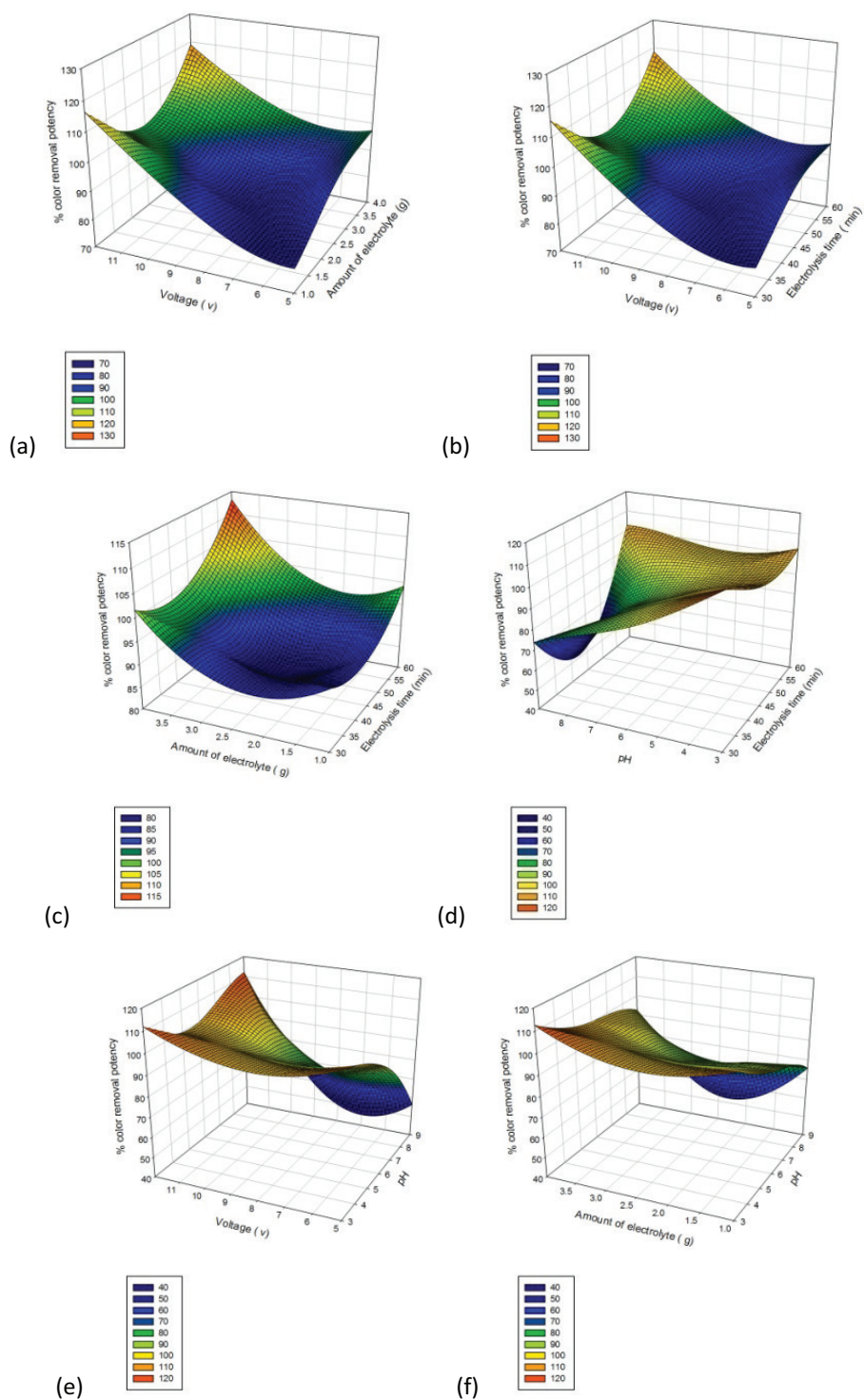
Fig. 2. The response surface plots of % removal efficiency of Y_3 (Blue 222).

higher by using NaCl represents the formation of hypochlorite. The effect of electrolyte concentration for the removal of tri-dyes system is represented in Figs. 2–4. The addition of electrolyte NaCl contributes the Cl⁻ ions which remove the insulating layer formed by Ca^{2+} and Mg^{2+} on the electrode and it doings as a good disinfectant [47,48].

3.3.4 The influence of the voltage

The influence of current (voltage) to EC reactor was observed to remove dyes. The greater the applied current density with respect to voltage changing, the more flocs were formed, and they interact with the dye molecules and enhanced the removal potency. In addition, it increases
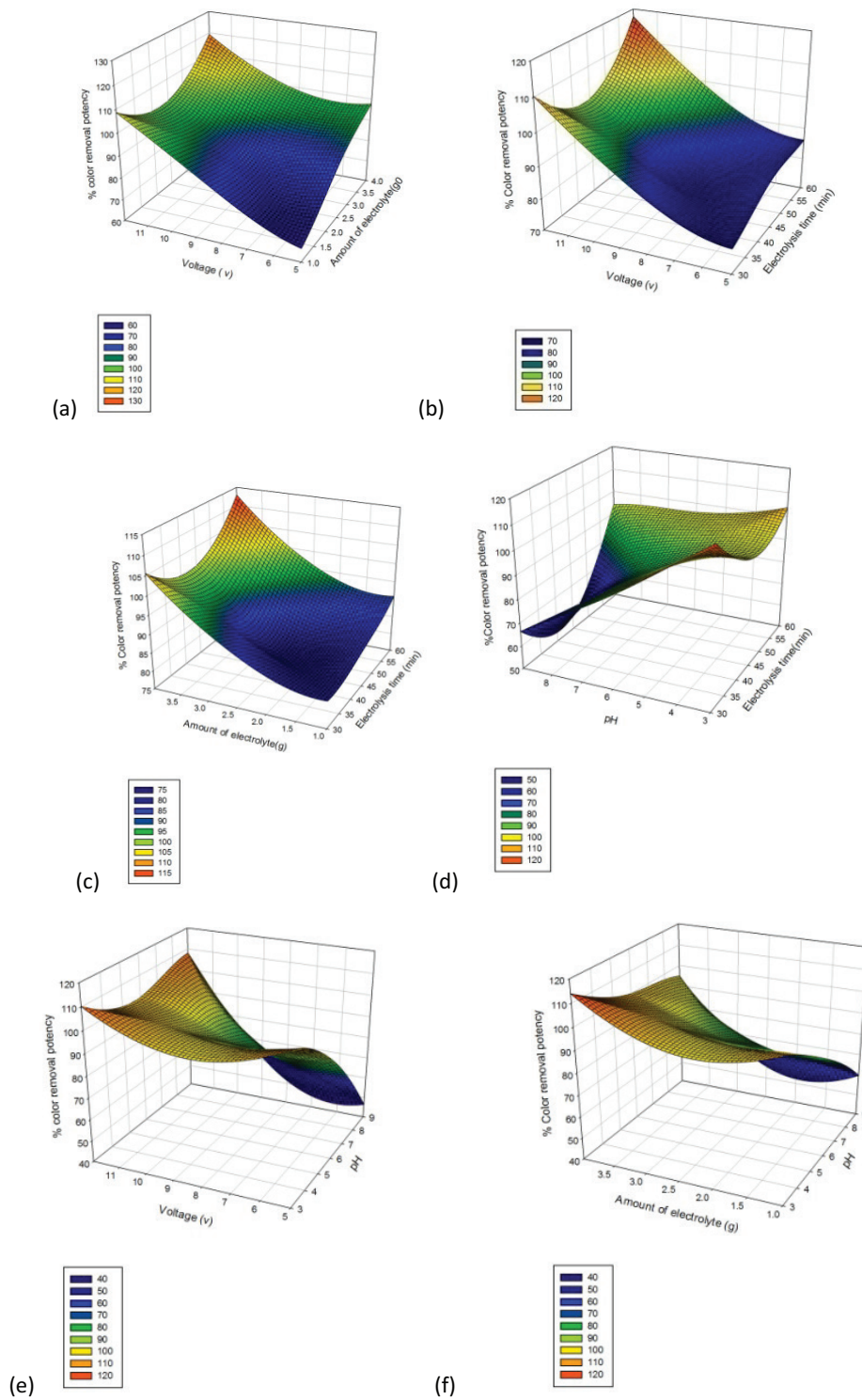
Fig. 3. The response surface plots of % removal efficiency Y_2 (RR195).

the oxidation and reduction of water which results to improve removal potency by flotation process. The magnitude of water electrolysis process changed the hydrogen ion concentration and observing the buffering of various parameter as shown in Figs. 2–4 [49,50].

3.4. Effect of variables on % COD removal potency

3.4.1. The influence of pH

The removal of chemical oxygen demand by EC process is owing to the pH values of the system. Furthermore, the

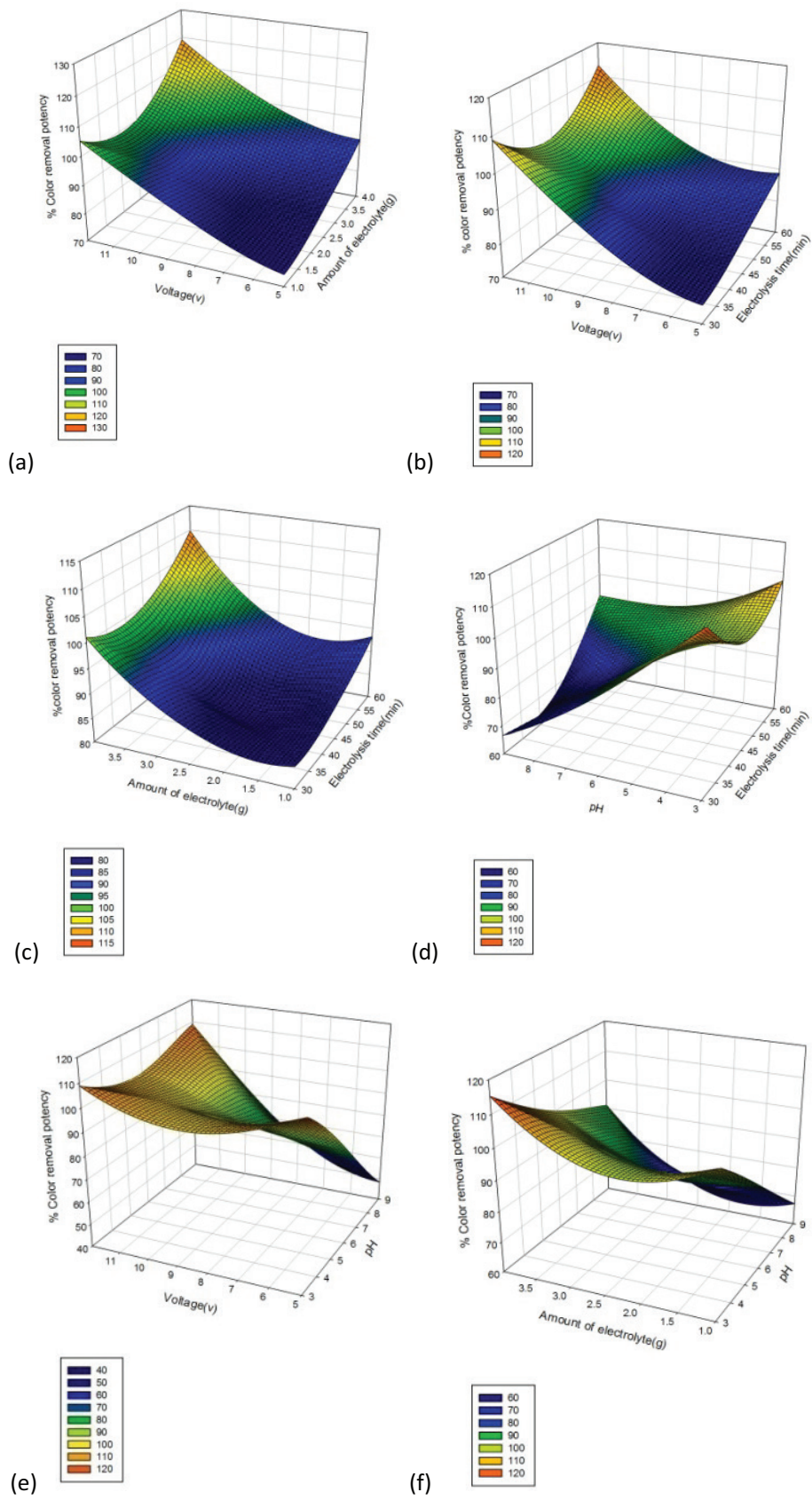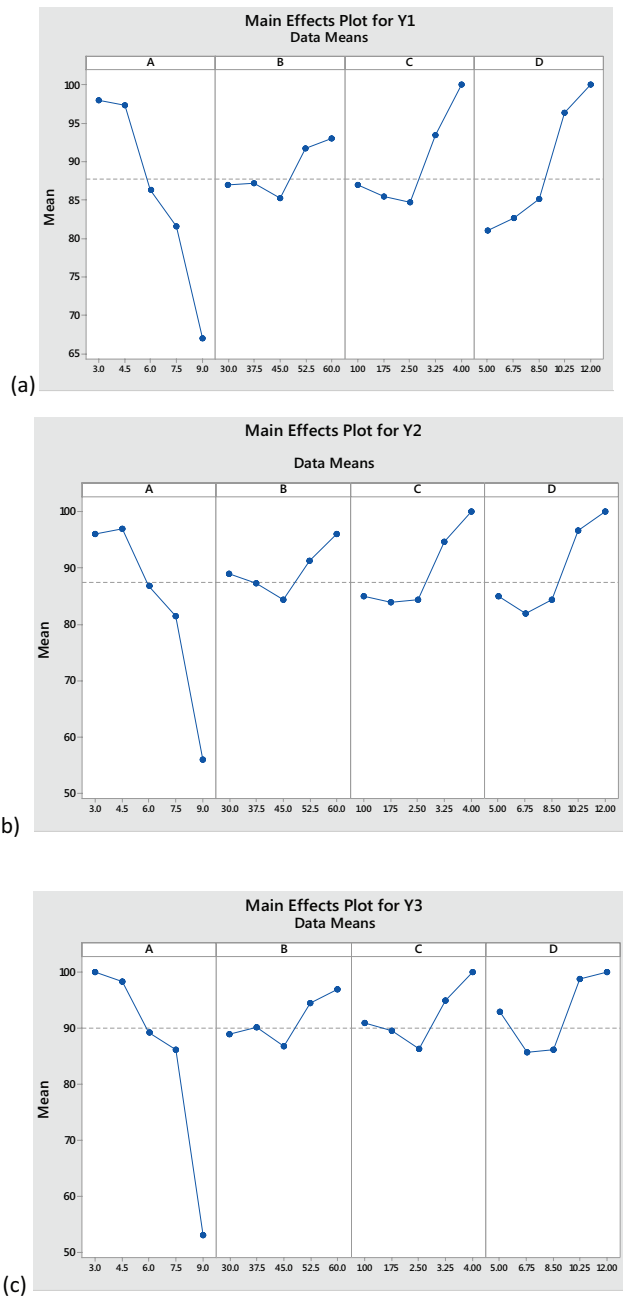Fig. 4. The response surface plots of % removal efficiency Y_1 (Y145).

(a)

(b)

(c)

Fig. 5. Main interaction effect plots of tri-dyes system of (a) Yellow 145 (b) Red 195 (c) Blue 222.

Table 4
The optimum operational parameters for the removal of dyes from tri-dyes system

Factors	Optimum values			
	$Y_{1=Yellow145}$	$Y_{2=Red195}$	$Y_{3=Blue\,222}$	% COD
A = pH	9	9	9	3
B = Electrolysis time(min)	60	60	30	60
C = Amount of electrolyte (g)	4	4	4	4
D = Voltage (v)	12	12	5	12
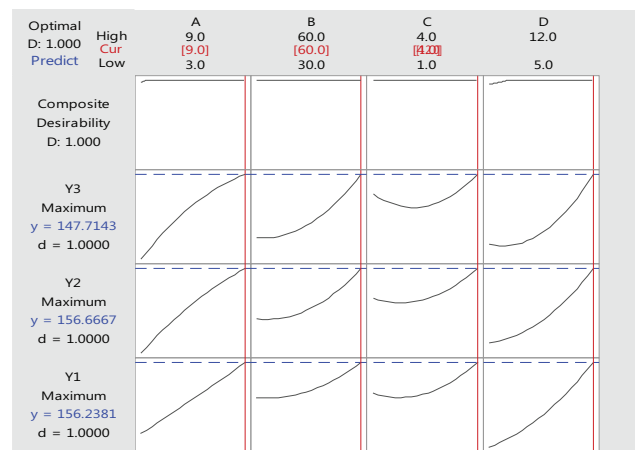
Fig. 6(a). The optimization plots for the % removal of respective tri-dyes system.
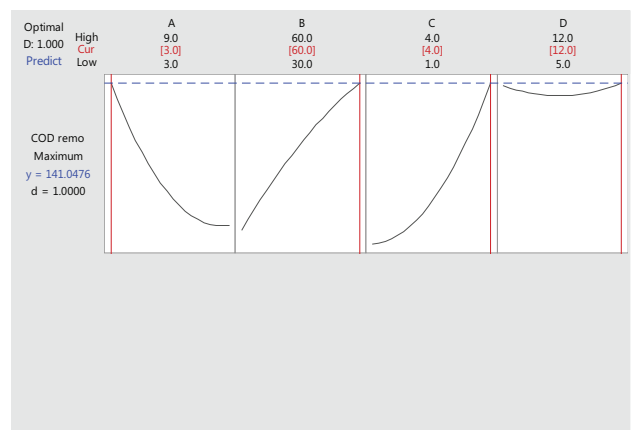
Fig. 6(b). The optimization plots for the % removal of COD.

increase in pH throughout the operation [39], for the determination of COD, the removal potency is larger at initial pH < 6, that dramatically falls at pH > 6. Furthermore, the buffering of the pH is considered beneficial throughout the process [51]. For each Al/Fe materials, it's cleared that COD removals show a similar trend.

3.4.2. The influence of amount of electrolyte

Fig. 7 portrays %COD removal that was increased by NaCl concentration. This could be contributed by addi-tional Cl$^-$ ions that act as good oxidizer, upon oxychloride (OCl$^-$) and Cl$_2$ gas production. As chloride particle scav-enges element to make OCl$^-$ ions at the electrode, and it reduces the passivation result and will increase the current efficiency [52]. The subsequent reactions justify the forma-tion of hypochlorite:

Fig. 7. Response surface plots of % COD removal efficiency as a function of operating parameters. (a) Electrolysis time (min), pH (b) Electrolysis time (min), Amount of electrolyte (g) (c) Amount of electrolyte (g), Voltage (V) (d) pH, Amount of electrolyte (g) (e) pH, Voltage (V) (f) Electrolysis time (min), Voltage (V).

$$2Cl^- \rightarrow Cl_2 + 2e^- \tag{15}$$

$$Cl_2 + H_2O \rightarrow HClO + H^+ + Cl^- \tag{16}$$

$$HClO \leftrightarrow ClO^- + H^+ \tag{17}$$

On the other hand, at higher concentration of NaCl, and improper dissolution of Al take place inflicting pollutants interaction between coagulator and pollutants [53].

3.4.3. The influence of electrolysis time

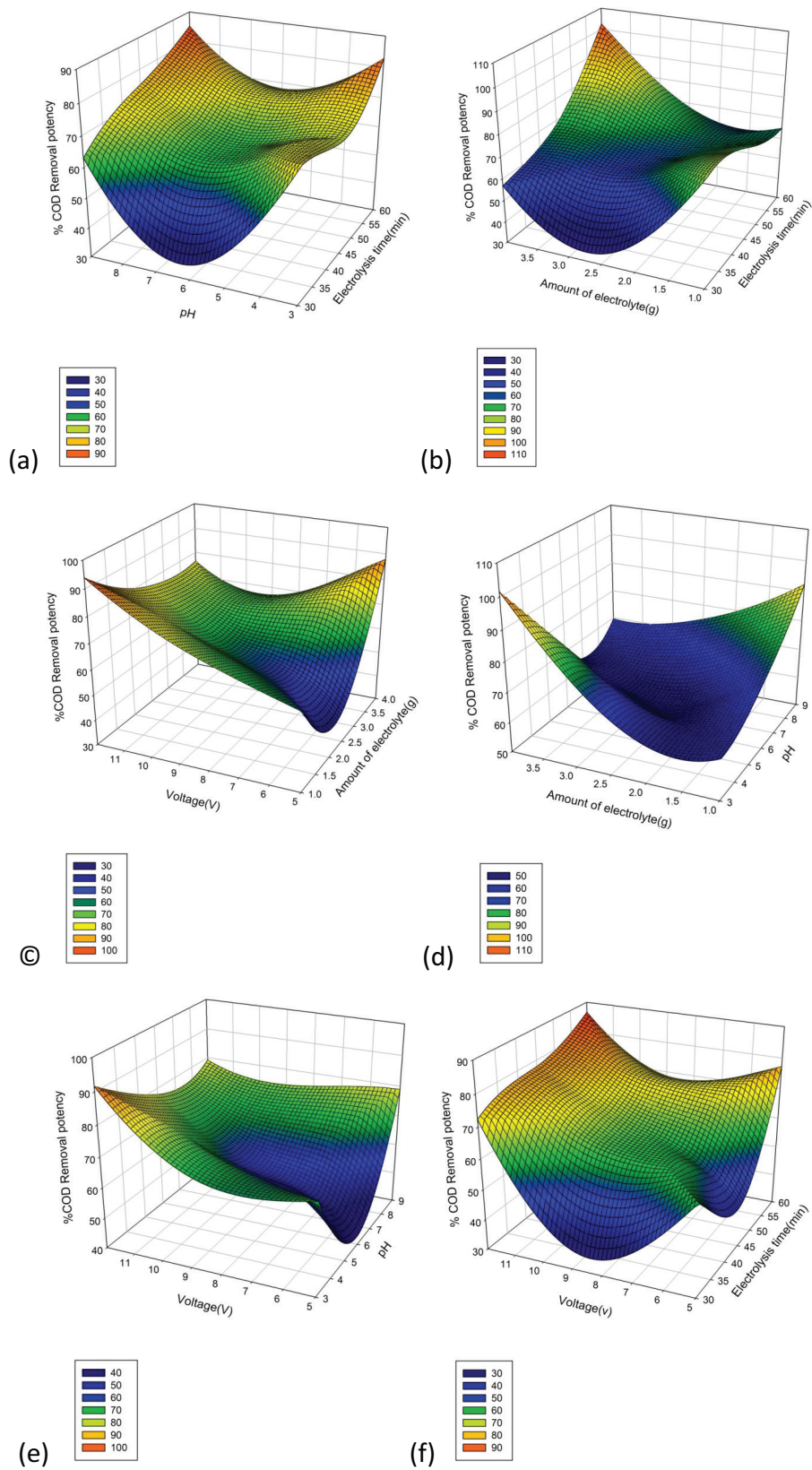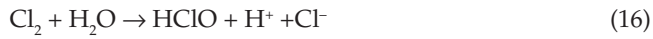If the electrolysis time is prolonged, then insoluble substances are conjointly decreases the conductivity of system. At that point, pollutants can lose their adsorption capacity and they will retar date the oxidation process at the anode. The oxidization capability of the electrodes at the interval of 15 min are going to be inadequate to oxidize the secondary pollutants and causes enhancement of anode passivation and resulted in higher electricity consumption. The result are shown in Fig. 7.

3.4.4. The influence of the voltage

At high voltage, due to hydrolysis of water, higher amount of coagulants are formed that result in increase in removal potency of pollutants [54]. Significantly, the COD removal rates were enhanced at high voltage, and secondary pollutants significantly were removed by the flocculation, flotation and oxidation method. The oxygen gas evolution increases at anode, due to high voltage [55,56].

3.5. Data analysis

3.5.1. Residual plots

The residuals are distributed and represented by normal probability plot as seen in Fig. 8. The values of coefficient of determination R^2 and their adjusted R^2 values are presented in model summary as represented in Table 5 for the removal of tri-dyes from the textile effluent. The estimated parameters and their implicit coded units. Moreover, the respective tables show the values of R^2 and their adjusted values. Furthermore, the P value indicates the statistical significance of the regression models. In addition, the P values are ($P < 0.05$) in response for regression model imply that second-order polynomial models was best fitted. Additionally, the R^2 values was 0.9161, 0.8983 and 0.8713 for the removal of Yellow145, Red195 and Blue 222. It expresses the higher correlation between the observed and predicted values.

3.5.2. Model fitting

The experimental response data were used to conduct a model using Response Surface Methodology (RSM). The
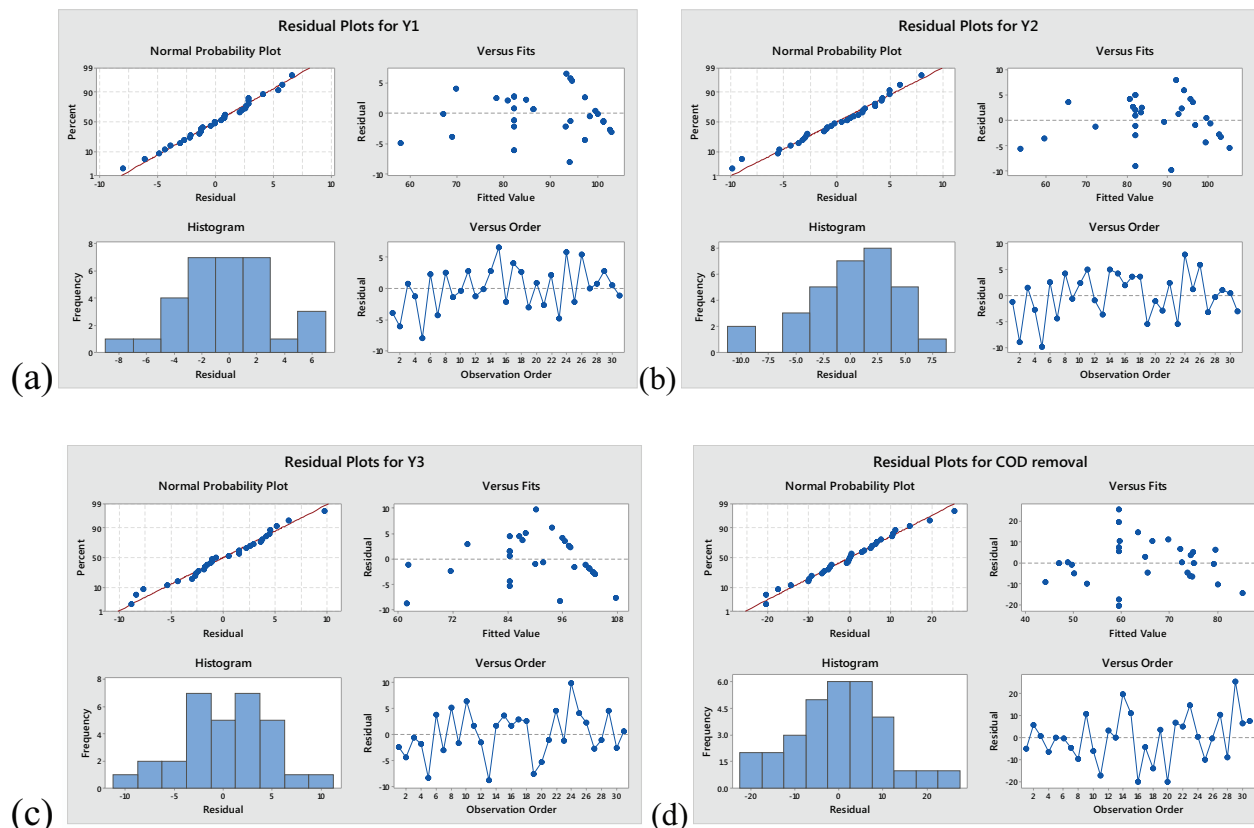

Fig. 8. The residual plots for % decolorization and % COD removal potency (a) Y_1 (Yellow 145) (b) Y_2 (Red 195) (c) Y_3 (Blue222) (d) % COD removal potency.

responses of % removal of dyes were correlated with the four factor variables, moreover, the response surface regression model was developed. The quadratic regression model equations are shown as Eqs. (18)–(21).

Table 5
Model summary of experimental design of EC process

Statistical parameters	Yellow 145	Reactive red 195	Blue 222.	% COD removal
$S_{\text{(Root Mean Square Error)}}$	4.790	5.860	5.900	14.98
R^2	0.916	0.898	0.871	0.501
$R^2_{\text{(Adj)}}$	0.843	0.809	0.759	0.065
$R^2_{\text{(pred)}}$	0.586	0.533	0.335	0.000

Table 6
The RSM model for the tri-dyes system

% Removal	Regression equation
Y_1 (Yellow 145)	Y1 = 395.8 − 41.02 A − 4.08 B − 25.7 C − 18.42 D + 0.067 A*A + 0.0360 B*B + 5.16 C*C + 0.703 D*D + 0.278 A*B + 1.22 A*C + 2.286 A*D + 0.000 B*C − 0.0667 B*D − 0.286 C*D(18)
Y_2 (Red 195)	Y2 = 425.1 − 36.9 A − 6.04 B − 16.9 C − 20.48 D − 0.602 A*A + 0.0493 B*B + 4.93 C*C + 0.905 D*D + 0.333 A*B + 2.11 A*C + 2.143 A*D − 0.022 B*C − 0.010 B*D − 1.52 C*D(19)
Y_3 (Blue 222)	Y3 = 402.9 − 30.1 A − 5.26 B − 24.1 C − 20.38 D − 0.737 A*A + 0.0438 B*B + 5.49 C*C + 1.091 D*D + 0.339 A*B + 0.94 A*C + 1.881 A*D + 0.100 B*C − 0.081 B*D − 1.19 C*D (20)
% COD removal	27 − 5.3 A − 0.34 B − 17.4 C + 11.2 D + 1.69 A*A − 0.0213 B*B + 6.31 C*C + 0.343 D*D + 0.106 A*B − 5.17 A*C − 0.79 A*D + 1.011 B*C − 0.024 B*D − 3.29 C*D(21)

Table 7
Analysis of variance for EC process

Component	Source	DF	Adj. SS	Adj. MS	F-value	p-value
Yellow145	Model	14	4010	286.5	12.48	0.000
	Error	16	367.3	22.95	*	*
	Lack-of-fit	10	298.4	29.84	2.600	0.127
	Pure error	6	68.86	11.48	*	*
	Total	30	4378	*	*	*
Reactive red195	Model	14	4852	346.5	10.10	0.000
	Error	16	549.0	34.32	*	*
	Lack-of-fit	10	403.1	40.31	1.660	0.277
	Pure error	6	146.0	24.33	*	*
	Total	30	5401	*	*	*
Blue222	Model	14	3887	277.6	7.730	0.000
	Error	16	574.3	35.90	*	*
	Lack-of-fit	10	496.6	49.66	3.830	0.057
	Pure error	6	77.71	12.95	*	*
	Total	30	4461	*	*	*
% COD removal	Model	14	3613	258.1	1.150	0.391
	Error	16	3592	224.6	*	*
	Lack-of-fit	10	1329	132.9	0.350	0.930
	Pure error	6	2263	377.3	*	*
	Total	30	7206	*	*	*

3.5.3. Analysis of variance (ANOVA)

Analysis of variance was carried out by quadratic model are presented in Table 7. The statistical parameters of regression, residual error and lack of fit and pure error and the p-value of ANOVA specifies the relationship between the response and the factors that are statistically significant at a level of $\alpha = 0.05$ (maximum acceptable level of risk for rejecting a true null hypothesis) [34]. The lack of fit F-test describes the variation in the data around the fitted model. If the model does not fit the data well, the lack of fit will be significant. The high p-value for lack of fit (>0.05) equals 0.127, 0.277 and 0.057 for dyes removal shows that the F-statistic was insignificant, implying significant model correlation between the factor variables and process response. Moreover, the ANOVA on this model, demonstrated that the model was highly significant, as evident from the 0.000 p-value in the regression.

Table 8
The estimated parameters and their implicit coded units

Component	Terms	Effect	Coef	SE Coef.	t-Value	P-Value	VIF
Yellow145	Constant		82.14	1.810	45.36	0.000	
	A	−15.67	−7.833	0.978	−8.010	0.000	1.00
	B	4.000	2.000	0.978	2.050	0.058	1.00
	C	7.500	3.750	0.978	3.830	0.001	1.00
	D	12.33	6.167	0.978	6.310	0.000	1.00
	A^2	0.304	0.152	0.896	0.170	0.868	1.03
	B^2	4.054	2.027	0.896	2.260	0.038	1.03
	C^2	5.804	2.902	0.896	3.240	0.005	1.03
	D^2	4.304	2.152	0.896	2.400	0.029	1.03
	AB	6.250	3.120	1.200	2.610	0.019	1.00
	AC	1.370	2.750	1.200	1.150	0.268	1.00
	AD	12.00	6.000	1.200	5.010	0.000	1.00
	BC	0.000	0.000	1.200	0.000	1.000	1.00
	BD	−1.750	−0.870	1.200	−0.730	0.476	1.00
	CD	−0.750	−0.370	1.200	−0.310	0.758	1.00
Reactive Red195	Constant		82.00	2.21	37.03	0.000	
	A	−17.00	−8.50	1.20	−7.11	0.000	1.00
	B	3.83	1.92	1.20	1.60	0.129	1.00
	C	9.67	4.83	1.20	4.04	0.001	1.00
	D	12.33	6.17	1.20	5.16	0.000	1.00
	A^2	−2.71	−1.35	1.10	−1.24	0.234	1.03
	B^2	5.54	2.77	1.10	2.53	0.022	1.03
	C^2	5.54	2.77	1.10	2.53	0.022	1.03
	D^2	5.54	2.77	1.10	2.53	0.022	1.03
	AB	7.50	3.75	1.46	2.56	0.021	1.00
	AC	4.75	2.37	1.46	1.62	0.124	1.00
	AD	11.25	5.62	1.46	3.84	0.001	1.00
	BC	−0.25	−0.13	1.46	−0.09	0.933	1.00
	BD	−0.25	−0.12	1.46	−0.09	0.933	1.00
	CD	−4.00	−2.00	1.46	−1.37	0.191	1.00
Blue222	Constant		84.43	2.26	37.28	0.000	
	A	−15.92	−7.96	1.22	−6.51	0.000	1.00
	B	4.25	2.13	1.22	1.74	0.101	1.00
	C	5.08	2.54	1.22	2.08	0.054	1.00
	D	9.92	4.96	1.22	4.05	0.001	1.00
	A^2	−3.32	−1.66	1.12	−1.48	0.158	1.03
	B^2	4.93	2.47	1.12	2.20	0.043	1.03
	C^2	6.18	3.09	1.12	2.76	0.014	1.03
	D^2	6.68	3.34	1.12	2.98	0.009	1.03
	AB	7.62	3.81	1.50	2.55	0.022	1.00
	AC	2.13	1.06	1.50	0.71	0.488	1.00
	AD	9.88	4.94	1.50	3.30	0.005	1.00
	BC	1.12	0.56	1.50	0.38	0.712	1.00
	BD	−2.12	−1.06	1.50	−0.71	0.488	1.00
	CD	−1.56	1.50	−3.12	−1.04	0.312	1.00

Continued

Table 8 (*Continued*)

%COD removal potency	Constant		59.43	5.660	10.49	0.000	
	A	0.420	0.210	3.060	0.070	0.947	1.000
	B	10.42	5.210	3.060	1.700	0.108	1.000
	C	1.080	0.540	3.060	0.180	0.862	1.000
	D	10.75	5.380	3.060	1.760	0.098	1.000
	A^2	7.600	3.800	2.800	1.360	0.194	1.030
	B^2	−2.40	−1.20	2.80	−0.43	0.674	1.030
	C^2	7.10	3.55	2.80	1.27	0.223	1.030
	D^2	2.10	1.05	2.80	0.37	0.713	1.030
	AB	2.37	1.19	3.75	0.32	0.755	1.000
	AC	−11.62	−5.81	3.75	−1.55	0.140	1.000
	AD	−4.13	−2.06	3.75	−0.55	0.590	1.000
	BC	11.37	5.69	3.75	1.52	0.148	1.000
	BD	−0.62	−0.31	3.75	−0.08	0.935	1.000
	CD	−8.62	−4.31	3.75	−1.15	0.267	1.000

Table 9
Effects of salt concentration on dyes removal, voltage drop, SEEC and total solid sludge. Initial dyes concentration: 30 mg/L

Salt (NaCl) Concentration (g/L)	Conductivity (mS/m)	Voltage drop (Volt)	Dye removal (%)	SEEC (KW h/ kg Al)	Sludge generated (kg/kg dye removed)	% Current efficiency	% Water recovery
1	3.12	0.5	100	1.813	1.19	154	92
2	5.41	1	100	2.060	1.93	134	91
3	5.75	0.9	100	1.626	2.92	123	87
4	4.49	3	100	1.562	3.65	111	83
5	5.67	3	100	0.759	3.87	123	81
6	6.12	4	100	0.597	4.16	110	82
7	7.56	5	100	0.303	4.12	125	79

3.5.4. Validation of model

Table 5 represents the response surface model which was developed in the current study with observed value of $R^2_{91.61(Yellow\ 145)}$ > $R^2_{(89.83\%\ Red\ 195)}$ > $R^2_{(87.13\ Blue\ 222)}$ respectively. Furthermore, the R^2_{adj} values were close to the R^2 value. It insures a satisfactory adjustment of the quadratic model to the experimental data. It is usually necessary to check the fitted model to ensure it provides an adequate approximation to the real system [33,34]. The normal probability plot is generally used to check the normal distribution of the residuals as shown in Fig. 8.

3.6. The specific electrical energy consumption and current efficiency

The Current efficiency (∅) for different operating conditions is calculated as [57]:

$$\varnothing = \frac{\Delta M_{experimental}}{\Delta M_{theoritical}} \times 100 \tag{22}$$

It is based on the comparison of experimental weight loss of Aluminum Electrodes M$_{experimental}$ during EC process with theoretical amount of Aluminum dissolution M$_{theoritical}$ according to the Faraday's law:

$$\Delta M_{theoritical=} \frac{M.I.t_{EC}}{\Delta n.F} \times 100 \tag{23}$$

where M is the atomic mass of the Al (g/mol), n is the number of electron moles, F is the Faraday constant (F = 96,487 C/mol) and t_{EC} is the time (s) of EC operation. Assuming Al(OH)$_{3(s)}$ is supposed to be the formed species the number of electron moles in dissolution reaction is equal to 3. The specific electrical energy consumption (SEEC) is calculated as a function of Al electrodes weight consumption during EC in kW h/(kg Al) [57].

$$SEEC = \frac{n \times F \times U}{3600 \times M \times} \tag{24}$$

In the present system, at the cathode surface change in over potential is not observed representing no precipitate formed on its surface. Indeed, the current efficiency values are shown in Table 9 [57,58–61].
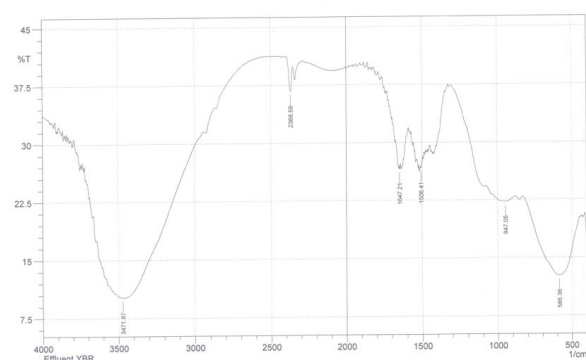
3.7. FTIR analysis of dyes

The FTIR spectrum of respective dyes, before and after EC process are shown in Fig. 9.

Table 10
Characterized bands in FTIR spectra for tridyes system

Functional groups	Wave number (cm^{-1})
OH, NH	3450.41
CH, Arom	<3000
C=C–	1481.23
N=N	1434.94
–C=N–	1587.31
C-N	1220.86
Sulfonates	1365–1340/1200–1100
Disulfides (CS stretch)	705–570
Sulfate ion	1130–1080/680–610
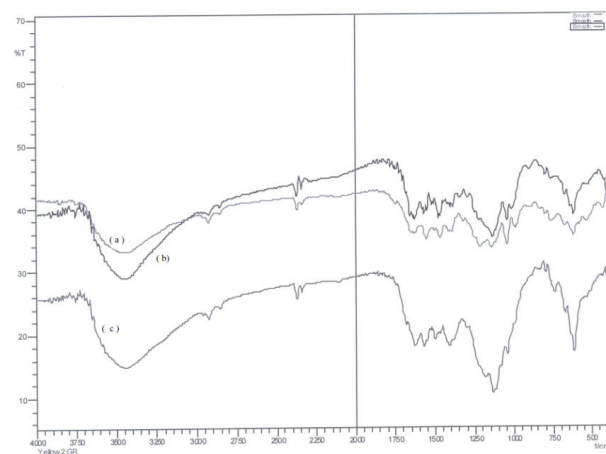
(A)

(B)

Fig. 9. (A) FTIR spectrum of dyes after adsorption (B) FTIR spectrum of pure dyes (a) Red195 (b) Blue222 (c) Yellow 145.

3.8. Kinetic study of EC system

The kinetics data of disappearance of tri-dyes is represented Table 11. Furthermore, the first order kinetic model was utilized which is represented as follows:

$$\ln[A]_t = \ln A_o - k \cdot t \qquad (25)$$

Table 11
Kinetic constants for first order model of dyes decolorization at (T: 23°C, NaCl: 4 g/L and V: 10 V, pH = 7, I = 0.58 A)

Effluent dyes	Kinetic model	Rate constant min^{-1}	$t_{1/2}$ (min)	R^2	Energy consumption (kwh)
Blue 222	First order	3.1×10^{-2}	22	0.954	2.13×10^{-3}
Red 195	First order	3.0×10^{-2}	32	0.866	3.09×10^{-3}
Yellow 145	First order	3.1×10^{-2}	31	0.903	2.99×10^{-3}

Table 12
The cost analysis at optimal conditions (Al electrode consumption = 1.488×10^{-3} kg/dm^3, NaCl = 4 g, Reaction time of 60 min, pH = 9, V = 12 volt)

Parameter	Quantity
Energy consumption (kwh/dm³)	0.019
Sodium chloride (kg/dm³)	0.01
Sodium hydroxide consumption (kg/dm³)	0.01
Sludge production (kg/dm³)	0.7
Electrode consumption (Kg/dm³)	1.488×10^{-3}
Hydrochloric acid (mL/dm³)	100
Dyes (kg/dm³)	7.5×10^{-4}
Electrical energy cost (US$/dm³)	3.2734×10^{-4}
Dye cost (US$/dm³)	0.126
Electrode cost (US$/dm³)	0.14
Hydrochloric acid cost (US$/dm³)	0.1
Hydroxide sodium cost (US$/dm³)	1
Sodium chloride (US$/dm³)	0.001
Total operating cost (US$/dm³)	1.360

3.9. Operating cost analysis

Energy, sacrificial electrodes and chemicals are used during the process and their costs are taken into account in the calculation of the operating cost, as US$ per dm^3 for the treatment of textile discharge wastewater. The following equation was used to estimate operating cost. The cost analysis at optimal conditions is given in Table 13.

$$\text{Operating cost} = aC_{energy} + bC_{electrode} + eC_{chemicals} \qquad (26)$$

where C_{energy}, $C_{electrode}$, C_{sludge}, $C_{chemicals}$, are represented as a, b, d, while the e represent the energy intake for every dm^3 of wastewater (kWh/dm^3).

4. Comparison between this work and previous work

The comparative work is represented in Table 13 to show the significance of EC process for the treatment of dye effluent discharges.

5. Conclusion

The results obtained in the present study, provides an opportunity for the application of the EC process as

Table 13
Electrocoagulation process used for removal of various type of dyes

Reference no	Dye	Current or current density	Anode-cathode	% Removal efficiency
62	Reactive orange 84	130 A/m²	Fe-Fe	66, 76
63a	Acid red131, Reactiveyellow 86, Indanthrene blue RS, Basic GR 4, Reactive yellow 145	0.0625 A/cm²	Al-Al	97
64b	Reactive black B, Orange 3R, Yellow GR	0.0625 A/cm²	Al-Al	98
65	Azo, Anthraquinone, Xanthene	0.3 A	Fe-Fe	98
66	Acid black 52, Acid yellow 220	40 A/m²	Al-Al	92, 95
67	Levafix brilliant blue E-B	100 A/cm²	Al-Al, Fe-Fe	99, 83
68	Acid, Reactive	4.0 mA/cm²	Fe-Carbon	95
69	Orange II	160 A/m²	Al-Al	94.5
70	Reactive black 5	4.575 mA/cm²	Fe-Fe	98.8
71	Reactive, Basic e	–	Al-Al, Fe-Fe	96, 85.6
72	Direct red 23	30 A/m²	Fe-Fe, Al-Al	>95
73	Levafix blue CA	35.5 mA/cm²	Fe-Fe	99.5
74	Bomaplex red CR-L	0.50 mA/cm²	Al-Al	99.1
This work	Y145, RR195, Blue222	1.0 A	Al-Fe	>80%

a purification technique of the textile industrial effluent. It showed higher removal efficiencies (>90%) of color removal potency at optimum conditions of dyes system. The EC process, at pH = 3, electrolysis time of 60 min, amount of electrolyte of 4 g, and voltage of 12 V applied to the wastewater yielded 84% of COD removal. After electrocoagulation study, COD, TDS, EC and hardness showed decrease in values which also indicated that the technique is best and more efficient to treat such type of effluents. In future, a combination of the EC process with other purification techniques, such as photochemsitry, adsorption and sonolysis would be accomplished for removal efficiency of organic substances. The author is intrigued for EC process for the treatment of effluent of intact Textile S.I.T.E zone (WEST), Karachi , Pakistan.

References

[1] A. Singh, T. Saraswathy, S.T. Ramesh, New trends in electrocoagulation for the removal of dyes from wastewater: A review, Environ. Eng. Sci., 30(7) (2013) 333–349.
[2] O.T. Can, M. Kobya, E. Demirbas, M. Bayramoglu, Treatment of the textile wastewater by combined electrocoagulation, Chemosphere, 62 (2006) 181–187.
[3] N. Daneshvar, A. Oladegaragoze, N. Djafarzadeh, Decolorization of basic dye solutions by electrocoagulation: an investigation of the effect of operational parameters, J. Hazard. Mater., B129 (2006) 116–122.
[4] P.C. Vandevivere, R. Bianchi, W. Verstraete, Treatment and reuse of wastewater from the textile wet-processing industry: Review of emerging technologies, J. Chem. Technol. Biotechnol., 72 (1998) 289–302.
[5] S. Papic, N. Koprivanac, A.L. Bozic, A. Metes, Removal of some reactive dyes from synthetic wastewater by combined Al(III) coagulation/carbon adsorption process, Dyes Pigments, 62 (2004) 291–298.
[6] M.A. Sanroma, M. Pazos, M.T. Ricart, C. Cameselle, Electrochemical decolourisation of structurally different dyes, Chemosphere, 57 (2004) 233–239.
[7] P. Saha, S. Chowdhury, S. Gupta, I. Kumar, Insight into adsorption equilibrium, kinetics and thermodynamics of Malachite Green onto clayey soil of Indian origin, Chem. Eng. J., 165 (2010) 874–882.
[8] W.T. Mook, M.A. Ajeel, M.K. Aroua, M. Szlachta, The application of iron mesh double layer as anode for the electrochemical treatment of Reactive Black 5 dye, J. Environ. Sci., 54 (2017) 184–195.
[9] G. Chen, Electrochemical technologies in wastewater treatment, Sep. Purif. Technol., 38 (2004) 11–41.
[10] S. Bellebi, S. Kach, A.Z. Bouyakou, Z. Derrich, Experimental investigation of chemical oxygen demand and turbidity removal from cardboard paper mill effluents using combined electrocoagulation and adsorption processes, Environ. Prog. Sustain. Energy., 31 (2012) 361–370.
[11] E. Keshmirizadeh, S. Yousefi, M.K. Rofouei, An investigation on the new operational parameter effective in Cr (VI) removal efficiency: A study on electrocoagulation by alternating pulse current, J. Hazard. Mater., 190(1) (2011) 119–124.
[12] N.V. Narayanan, M. Ganesan, Use of adsorption using granular activated carbon (GAC) for the enhancement of removal of chromium from synthetic wastewater by electrocoagulation, J. Hazard. Mater., 161 (2009) 575–580.
[13] J. Nouri, A.H. Mahvi, E. Bazrafshan, Application of electrocoagulation process in removal of zinc and copper from aqueous solutions by aluminum electrodes, Int. J. Environ. Res., 4 (2010) 201–208.
[14] M.Y.A. Mollah, R. Schennach, J.P. Parga, D.L. Cocke, Electrocoagulation(EC)-science and applications, J. Hazard. Mater., B 84 (2001) 29–41.
[15] A.H. El-Shazly, A.A. AlZahrani, S.S. AlShahrani, Improvement of NO_3^- removal from wastewater by using batch electrocoagulation unit with vertical monopolar aluminum electrodes, Int. J. Electrochem. Sci., 6 (2011) 4141–4149.
[16] M.Y.A. Mollah, P. Morkovsky, J.A.G. Gomes, M. Kesmez, J. Parga, D.L. Cocke, Fundamentals, present and future perspectives of electrocoagulation, J. Hazard. Mater., 114 (2004) 199–210.

[17] S. Adamovic, M. Prica, B. Dalmacija, S. Rapajic, D. Nova-kovic, Z. Pavlovic, S. Maletic, Feasibility of electrocoagulation/flotation treatment of waste offset printing developer based on the response surface analysis, Arab. J. Chem., 9(1) (2016) 152–162.

[18] P. Canizares, M. Carmona, J. Lobato, F. Martinez, M.A. Rodrigo, Electro-dissolution of aluminum electrodes in electrocoagulation processes, Ind. Eng. Chem. Res., 44 (2005) 4178–4185.

[19] P. Canizares, C. Jimenez, F. Martinez, C. Saez, M.A. Rodrigo, Study of the electro-coagulation process using aluminium and iron electrodes, Ind. Eng. Chem. Res., 46 (2007) 6189–6195.

[20] A.K. Chopra, A.K. Sharma, Removal of turbidity, COD and-BOD from secondarily treated sewage water by electrolytic treatment, Appl. Water Sci., 3 (2013)125–132.

[21] I. Zongo, A.H. Maiga, J. Wéthé, G. Valentin, J.-P. Leclerc, G. Paternotte, F. Lapicque, Electrocoagulation for the treatment of textile wastewaters with Al or Fe electrodes: compared variations of COD levels, turbidity and absorbance, J. Hazard. Mater., 169 (2009) 70–76.

[22] I. Heidmann, W. Calmano, Removal of Zn(II), Cu(II), Ni(II), Ag(I) and Cr(VI) present in aqueous solutions by aluminium electrocoagulation, J. Hazard. Mater., 152 (2008) 934–941.

[23] G. Mouedhen, M. Feki, M. DePetrisWery, H.F. yedi, Behavior of aluminum electrodes in electrocoagulation process, J. Hazard. Mater., 150 (2008) 124–135.

[24] G. Mouedhen, M. Feki, M.D. Petris-Wery, H.F. Ayedi, Electrochemical removal of Cr(VI) from aqueous media using iron and aluminum as electrode materials: Towards a better understanding of the involved phenomena, J. Hazard. Mater., 168 (2009) 983–991.

[25] A. Fakhri, Investigation of mercury (II) adsorption from aqueous solution onto copper oxide nanoparticles: optimization using response surface methodology, Process. Saf. Environ., 93 (2015) 1–8.

[26] J.S. Do, M.L. Chen, Decolourization of dye-containing solutions by electrocoagulation, J. Appl. Electrochem., 24 (1994) 785–790.

[27] APHA, 1992. Standard methods for examination of water and wastewater. American Water Work Association, New York.

[28] S.K. Maiti, Handbook of Methods in Environmental Studies (1 and 2), ABD Publishers, Jaipur, 2004.

[29] M. Casillas, A. Hector, Electrocoagulation mechanism for COD removal, Sep. puri. Techn., 56 (2007) 204–211.

[30] T.H. Kim, C. Park, E.B. Shin, S. Kim, Decolorization of disperse and reactive dyes by continuous electrocoagulation process, Desalination, 150 (2002) 165–175.

[31] M.S. Secula, I. Crețescu, S. Petrescu, An experimental study of indigo carmine removal from aqueous solution by electrocoagulation, Desalination, 277 (2011) 227–235.

[32] E. Gengec, M. Kobya, E. Demirbas, A. Akyol, K. Oktor, Optimization of baker's yeast wastewater using response surface methodology by electrocoagulation, Desalination, 286 (2012) 200–209.

[33] A. Dean, D. Voss, Design and Analysis of Experiments, Springer-Verlag, New York, 1999.

[34] D.C. Montgomery, Design and Analysis of Experiments, 6thed., John Wiley & Sons Inc., New York, 2005.

[35] A.I. Khuri, S. Mukhopadhyay, Response surface methodology, WIREs Computational Statistics, 2 (2010) 128–149.

[36] R.-M. Gabriela, E.C-. Medina, J.A-. Cotero, B. Bilyeu, C.B-. Díaz, Aluminum electrocoagulation with peroxide applied to wastewater from pasta and cookie processing, Sep. Purif. Technol., 54(1) (2007) 124–129.

[37] M. Kobya, O.T. Can, M. Bayramoglu, Treatment of textile wastewaters by electrocoagulation using iron and aluminum electrodes, J. Hazard. Mater., B100 (2003) 163–178.

[38] A. Gurses, M. Yalcin, C. Dogar, Electrocoagulation of some reactive dyes: a statistical investigation of some electrochemical variables, Waste. Manag., (2002) 22491–22499.

[39] O.T. Can, M. Bayramoglu, M. Kobya, Decolorization of reactive dye solutions by electrocoagulation using aluminum electrodes, Ind. Eng. Chem. Res., 42 (2003) 3391–3396.

[40] X. Chen, G. Chen, P.L. Yue, Separation of pollutants from restaurant wastewater by electrocoagulation, Sep. Purif. Technol., 19 (2000) 153.

[41] E.A. Vik, D.A. Carlson, A.S. Eikum, E.T. Gjessing, Electrocoagulation of potable water. Water Res., 18 (1984) 1355.

[42] R. Katal, H. Pahlavanzadeh, Influence of different combinations of aluminum and iron electrode on electrocoagulation efficiency: application to the treatment of paper mill wastewater, Desalination, 265 (2011) 199–205.

[43] M. Eyvaz, M. Kirlaroglu, T.S. Aktas, E. Yuksel, The effects of alternating current electrocoagulation on dye removal from aqueous solutions, Chem. Eng. J., 153 (2009) 16–22.

[44] C.A. Martínez-Huitle, E. Brillas, Decontamination of wastewaters containing synthetic organic dyes by electrochemical methods: a general review, App. Catalysis B: Environ., 87 (2009) 105.

[45] S. Aber, A.R. Amani-Ghadim, V. Mirzajani, Removal of Cr(VI) from polluted solutions by electrocoagulation: modeling of experimental results using artificial neural network, J. Hazard. Mater., 171 (2009) 484–490.

[46] Y.S. Yildiz, A.S. Koparal, S. Irdemez, B. Keskinler, Electrocoagulation of synthetically prepared waters containing high concentration of NOM using iron cast electrodes, J. Hazard. Mater., B139 (2007) 373–380.

[47] C. Raghavacharya, Color removal from industrial effluents—A comparative review of available technologies, Chem. Eng. World., 32 (1997) 53.

[48] H.M. Wong, C. Shang, Y.K. Cheung, G. Chen, Chloride assisted electrochemical disinfection. In Proceedings of the Eighth Mainland-Taiwan Environmental Protection Conference, Tsin Chu, Taiwan., (2002).

[49] C. Saez, P. Canizares, F. Martinez, M.A. Rodrigo, Improving the efficiencies of batch coagulation processes with small modifications in the pH, Sep. Sci. Technol., 45 (2010) 1411–1417.

[50] P. Canizares, C. Jimenez, F. Martinez, M.A. Rodrigo, C. Saez, The pH as a key parameter in the choice between coagulation and electrocoagulation for the treatment of wastewaters, J. Hazard. Mater., 163 (2009) 158–164.

[51] S. Bebelis, K. Bouzek, A. Cornell, M.G.S. Ferreira, G.H. Kelsall, F. Lapicque, C.P. deLeon, M.A. Rodrigo, F.C. Walsh, Highlights during the development of electrochemical engineering, Chem. Eng. Res. Des., 91 (2013) 1998–2020.

[52] R. Sridhar, V. Sivakumar, V.P. Immanuel, J.P. Maran, Treatment of pulp and paper industry bleaching effluent by electrocoagulant process, J. Hazard. Mater., 186 (2011) 1495–1502.

[53] S.H. Lin, C.F. Peng, Treatment of textile wastewater by electrochemical method, Water. Res., 28 (1994) 277–282.

[54] C. Wang , D.Q. Zhang, Y.Z. Chen, Study of the relation between electric current density and cell voltage in the process of electrocoagulation, Industrial Water Treatment, 22(7) (2002) 28–30.

[55] J. Ge, J. Qu , P. Lei, H. Liu, New bipolar electrocoagulation–electroflotation process for the treatment of laundry wastewater, Sep. Purif. Technol., 36 (2004) 33–39.

[56] X. Chen, G. Chen, P.L. Yue, Separation of pollutants from restaurant wastewater by electrocoagulation, Sep. Purif. Technol., 19 (2000) 65–76.

[57] D. Ghosh, C.R. Medhi, M.K. Purkait, Treatment of fluoride contaminated drinking water by electrocoagulation using monopolar and bipolar electrode connection, Chemosphere, 73 (2008) 1393–1400.

[58] F. Shen, P. Gao, X. Chen, G. Chen, Electrochemical removal of fluoride ions from industrial wastewater, Chem. Eng. Sci., 58 (2003) 987–993.

[59] N. Mameri, A.R. Yeddou, H. Lounici, D. Belhocine, H. Grib, B. Bariou, Defluoridation of septentrional Sahara water of North Africa by electrocoagulation process using bipolar aluminium electrodes, Water. Res., 32 (1998) 1604–1612.

[60] J.C. Donini, J. Kan, J. Szynkarczuk, T.A. Hassan, K.L. Kar, The operating cost of electrocoagulation, Can. J. Chem. Eng., 72 (1994) 1007–1012.

[61] L.S. Calvo, J.P. leclerc, G. Tanguy, M.C. Cames, G. Paternotte, G. Valentin, A. Rostan, F. Lapicque, An electrocoaguhtion unit for the purification of soluble oil wastes of high COD, Environ. Prog., 22 (2003) 57–65.

[62] E. Yuksel, M. Eyvaz, E. Gurbulak, Electrochemical treatment of colour index Reactive Orange 84 and textile wastewater by using stainless steel and iron electrodes, Environ. Prog. Sust. Energy., 32(1) (2013) 60–68.

[63] V. Khandegar, A.K. Saroha, Electrochemical treatment of effluent from small scale dyeing unit, Indian. Chem. Eng., 55(2) (2013a) 1–9.

[64] V. Khandegar, A.K. Saroha, Electrochemical treatment of textile effluent containing Acid Red 131 dye, J. Hazard. Toxic. Radio. Waste., 2013b (in press).

[65] M.C. Wei, K.S. Wang, C.L. Huang, C.W. Chiang, T.J. Chang, S.S. Lee, S.H. Chang, Improvement of textile dye removal by electrocoagulation with low-cost steel wool cathode reactor, Chem. Eng. J., 192 (2012) 37–44.

[66] E. Pajootan, M. Arami, N.M. Mahmoodi, Binary system dye removal by electrocoagulation from synthetic and real colored wastewaters, J. Taiwan. Inst. Chem. Eng., 43(2) (2012) 282–290.

[67] F. Akbal, A. Kuleyin, Decolorization of Levafix Brilliant Blue E-B by electrocoagulation method, Environ. Prog. Sust. Energy., 30(1) (2011) 29–36.

[68] B.K. Korbahti, A. Tanyolac, Electrochemical treatment of simulated textile wastewater with industrial components and Levafix Blue CA reactive dye: optimization through response surface methodology, J. Hazard. Mater., 151(2–3) (2008) 422–431.

[69] M.Y.A. Mollah, J.A.G. Gomes, K.K. Das, D.L. Cocke, Electrochemical treatment of Orange II dye solution use of aluminum sacrificial electrodes and floc characterization, J. Hazard. Mater., 174(1–3) (2010) 851–858.

[70] I.A. Sengil, M. Ozacar, The decolorization of C.I. Reactive Black 5 in aqueous solution by electrocoagulation using sacrificial iron electrodes, J. Hazard. Mater., 161(2–3) (2009) 1369–1376.

[71] K. Charoenlarp, W. Choyphan, Reuse of dye wastewater through colour removal with electrocoagulation process, Asian. J. Energy. Environ., 10(4) (2009) 250–260.

[72] C. Phalakornkule, S. Polgumhang, W. Tongdaung, Performance of an electrocoagulation process in treating direct dye: batch and continuous up flow processes, World. Acad. Sci. Eng. Technol., 57 (2009) 277–282.

[73] B.K. Korbahti, A. Tanyolac, Electrochemical treatment of simulated textile wastewater with industrial components and Levafix Blue CA reactive dye: optimization through response surface methodology, J. Hazard. Mater., 151(2–3) (2004) 22–431.

[74] Y.S. Yildiz, Optimization of Bomaplex Red CR-L dye removal from aqueous solution by electrocoagulation using aluminum electrodes, J. Hazard. Mater., 153(1–2) (2008) 194–200.